

Deletion of SIRT6 in vascular smooth muscle cells facilitates vascular calcification via suppression of DNA damage repair

Siyi Wang^{a,1}, Li Li^{b,1}, Qingchun Liang^{c,1}, Yuanzhi Ye^a, Zirong Lan^a, Qianqian Dong^a, An Chen^a, Mingwei Fu^a, Yining Li^a, Xiaoyu Liu^a, Jing-Song Ou^d, Lihe Lu^{e,*}, Jianyun Yan^{a,*}

^a Department of Cardiology, Laboratory of Heart Center, Heart Center, Zhujiang Hospital, Southern Medical University; Guangdong Provincial Key Laboratory of Cardiac Function and Microcirculation; Guangdong Provincial Biomedical Engineering Technology Research Center for Cardiovascular Disease, Guangzhou 510280, China

^b Department of Cardiology, Guangzhou Red Cross Hospital, Jinan University, Guangzhou 510220, China

^c Department of Anesthesiology, The Third Affiliated Hospital, Southern Medical University, Guangzhou 510665, China

^d Division of Cardiac Surgery, National-Guangdong Joint Engineering Laboratory for Diagnosis and Treatment of Vascular Diseases, NHC key Laboratory of Assisted Circulation, The First Affiliated Hospital, Sun Yat-sen University, Guangzhou 510080, China

^e Department of Pathophysiology, Zhongshan Medical School, Sun Yat-Sen University, Guangzhou 510080, China

ARTICLE INFO

Keywords:

Vascular calcification
Vascular aging
DNA damage
SIRT6
ATM
Vascular smooth muscle cells

ABSTRACT

Vascular calcification is an important risk factor for cardiovascular events, accompanied by DNA damage during the process. The sirtuin 6 (SIRT6) has been reported to alleviate atherosclerosis, which is related to the reduction of DNA damage. However, whether smooth muscle cell SIRT6 mediates vascular calcification involving DNA damage remains unclear. Western blot and immunofluorescence revealed that SIRT6 expression was decreased in human vascular smooth muscle cells (HVSMCs), human and mouse arteries during vascular calcification. Alizarin red staining and calcium content assay showed that knockdown or deletion of SIRT6 significantly promoted HVSMC calcification induced by high phosphorus and calcium, accompanied by upregulation of osteogenic differentiation markers including Runx2 and BMP2. By contrast, adenovirus-mediated SIRT6 overexpression attenuated osteogenic differentiation and calcification of HVSMCs. Moreover, *ex vivo* study revealed that SIRT6 overexpression inhibited calcification of mouse and human arterial rings. Of note, smooth muscle cell-specific knockout of SIRT6 markedly aggravated Vitamin D₃-induced aortic calcification in mice. Mechanistically, overexpression of SIRT6 reduced DNA damage and upregulated p-ATM during HVSMCs calcification, whereas knockdown of SIRT6 showed the opposite effects. Knockdown of ATM in HVSMCs abrogated the inhibitory effect of SIRT6 overexpression on calcification and DNA damage. This study for the first time demonstrates that vascular smooth muscle cell-specific deletion of SIRT6 facilitates vascular calcification via suppression of DNA damage repair. Therefore, modulation of SIRT6 and DNA damage repair may represent a therapeutic strategy for vascular calcification.

Abbreviations: α -SMA, alpha smooth muscle actin; γ H2AX, phosphorylation of histone H2AX on serine 139; ALP, alkaline phosphatase; ATM, ataxia telangiectasia mutation; BMP2, bone morphogenetic protein-2; CHD4, Chromatin helicase DNA binding protein 4; CM, calcifying medium; DDR, DNA damage response; DSBs, double-strand breaks; GM, growth medium; HVSMCs, human vascular smooth muscle cells; MVSMCs, mouse vascular smooth muscle cells; NAM, nicotinamide; p-ATM, phosphorylation of ataxia telangiectasia mutation at Ser1981; Runx2, Runt-related transcription factor 2; SIRT1, sirtuin 1; SIRT6, sirtuin 6; SMM-HC, smooth muscle myosin heavy chain; SM22 α , smooth muscle 22 alpha; VitD₃, vitamin D₃; VSMCs, vascular smooth muscle cells.

* Correspondence to: J. Yan, Department of Cardiology, Heart Center, Zhujiang Hospital, Southern Medical University, 253 Industrial Avenue, Guangzhou 510280, China.

** Correspondence to: L. Lu, Department of Pathophysiology, Zhongshan School of Medicine, Sun Yat-Sen University, 74 Zhongshan Er Road, Guangzhou 510080, China.

E-mail addresses: lulihe@mail.sysu.edu.cn (L. Lu), yanjy790@smu.edu.cn (J. Yan).

¹ These authors contributed equally to this work.

<https://doi.org/10.1016/j.yjmcc.2022.10.009>

Received 31 May 2022; Received in revised form 23 September 2022; Accepted 25 October 2022

Available online 29 October 2022

0022-2828/© 2022 Elsevier Ltd. All rights reserved.

1. Introduction

Vascular calcification, a common complication of atherosclerosis, diabetes, aging, and chronic kidney disease, is associated with cardiovascular events and mortality [1–3]. Abnormal deposition of calcium and phosphate minerals in vessel wall, similar to bone formation, is the etiology of vascular calcification [4,5]. Previous studies have demonstrated that vascular smooth muscle cells (VSMCs) play an important role in the process of vascular calcification through transition from contractile to osteogenic phenotype [6]. In response to various stimuli such as calcium and phosphate disorder, hyperglycemia, inflammation, oxidative stress and DNA damage, VSMCs undergo osteogenic differentiation and upregulate the expression of osteogenic proteins, such as runt-related transcription factor 2 (Runx2), bone morphogenetic protein-2 (BMP2) and alkaline phosphatase (ALP), and down-regulate the expression of contractile protein, such as alpha smooth muscle actin (α -SMA), smooth muscle myosin heavy chain (SMM-HC), smooth muscle 22 alpha (SM22 α) [7–10]. Senescent VSMCs have been shown to promote vascular calcification by increasing osteogenic differentiation and upregulating Runx2 and ALP expression [11]. Moreover, vascular aging is associated with telomere erosion and DNA damage, accompanied by the decrease of DNA repair ability [12]. Several studies have reported that DNA damage exists in the process of vascular calcification, and it can promote calcification [13,14]. DNA damage could be a common mechanism underlying vascular calcification and vascular aging. Therefore, repairing DNA damage may become an effective strategy for the prevention and treatment of vascular calcification and aging.

DNA damage response (DDR) is a highly orchestrated process that can be activated by DNA damage [15]. The most severe type of DNA damage is double-strand breaks (DSBs). Ataxia-telangiectasia mutated (ATM) is activated in response to DSBs in which ATM dissociates from dimers and then autophosphorylates at Ser1981 [16,17]. Then activated ATM leads to the activation of downstream effector molecules of DDR, such as checkpoint kinases, p53 and p21, which contribute to an arrest in the cell cycle, followed by DNA repair or apoptosis or senescence [18,19]. Furthermore, H2AX could be phosphorylated at Ser139 (γ -H2AX) by these molecules recruited by DNA damage, and γ -H2AX acts as a DNA damage marker and serves as a platform for locating repair proteins near DSBs [20,21]. Previous studies have demonstrated that p-ATM and γ -H2AX expression is upregulated during vascular calcification [22,23]. Activation of ATM has been reported to reduce DNA damage and extend lifespan in progeria mice [18], and to initiate DDR and repair damaged DNA in a variety of tumor cells [24,25]. However, the regulatory mechanism underlying DNA damage and DDR involved in vascular calcification remains unclear.

Sirtuin 6 (SIRT6), a NAD⁺ dependent class IV histone deacetylase, is involved in the regulation of inflammation [26], oxidative stress [27], DNA damage repair [28] and energy metabolism [29,30] in various diseases. SIRT6 mediates the regulation of various DNA damage repairs, including base excision [31], single-strand break repair [31], DSBs repair [28,32], and telomere integrity [33,34]. Recently, SIRT6 has been demonstrated as a DNA damage sensor to directly recognize DSBs and initiate the subsequent DDR [35,36]. SIRT6 prolongs lifespan and ameliorates cellular senescence and aging-related cardiovascular diseases [37]. In vascular system, SIRT6 plays a pivotal role in hypertension [38], vascular inflammation [39,40], vascular aging and atherosclerosis [34,41,42]. However, the role of smooth muscle cell SIRT6 in vascular calcification and the link between SIRT6 and DNA damage repair during vascular calcification have yet to be elucidated. In this study, we used smooth muscle cell-specific knockout of SIRT6 mouse model to investigate whether and how loss of SIRT6 in VSMCs contributes to vascular calcification.

2. Experimental procedures

2.1. Animals

All animal experiments in this study were performed in accordance with the National Institutes of Health's Guidelines for the Care and Use of Laboratory Animals and were approved by the Institutional Animal Care and Use Committee at Zhujiang Hospital, Southern Medical University, China (LAEC-2021-043). Male C57BL/6 J mice were purchased from Central Animal Care Facility of Southern Medical University. SIRT6 floxed (SIRT6^{f/f}) mice (Stock No. 017334) and SM22 α -Cre transgenic mice (Stock No. 004746) were obtained from the Jackson Laboratory (Bar Harbor, ME, USA). SIRT6^{f/f} mice were crossed to SM22 α -Cre transgenic mice to generate SM22 α -Cre:SIRT6^{f/+} heterozygous mice and they were further crossed to SIRT6^{f/f} mice to obtain SM22 α -Cre: SIRT6^{f/f} (designated as SIRT6 conditional knockout, CKO). SIRT6^{f/f} mice were used as wild type (WT) controls. All mice were housed in standard laboratory conditions with a 12 h light /12 h dark cycle and had free access to tap water and food. Male WT and CKO mice were randomly divided into two groups, including Control (Vehicle, $n = 6$), Model (Vitamin D₃, VitD₃, $n = 6$). Mice in model groups were subcutaneously injected with VitD₃ (Sigma Aldrich, 5×10^5 IU/kg) for 3 consecutive days and then fed with chow diet for another 6 days, as described in our previous studies [43,44]. At the end of the experiment, the animals were sacrificed and aortas were collected for further analysis.

2.2. Genomic PCR

Genomic DNA was prepared from mouse tails. Tails were lysed with lysis buffer (10 mM Tris HCl, 10 mM EDTA, 0.5% SDS, 10 mM NaCl and 100 μ g/ml proteinase K) overnight at 55 °C and 150 rpm. The sample was mixed with DNA extraction phenol reagent (Solarbio, Beijing, China) and centrifuged for 5 min to obtain supernatant with DNA. The supernatant was precipitated with absolute ethanol, washed with 70% ethanol and dissolved in deionized water. All mice were amplified with 2 \times Taq Master Mix (Vazyme Biotech, Nanjing, China) and specific primers. Finally, the genotypes were validated by agarose gel electrophoresis. The primers were as follows: SIRT6 (forward 5'-3'): AGTGAGGGGCTAATGGGAAC, SIRT6 (reverse 5'-3'): AACCCACCTCTCTCCCCTAA, SM22 α -Cre (forward 5'-3'): GCGGTCTGGCAGTAAAACTATC, SM22 α -Cre (reverse 5'-3'): GTGAAACAGCATTGTGCTCACTT.

2.3. Cell culture

Human vascular smooth muscle cells (HVSMCs) were purchased from American type culture collection (ATCC, CRL-1999, Manassas, VA, USA) and cultured in growth medium (GM) in an incubator with 5% CO₂ at 37 °C. GM was composed of DMEM (Gibco, Life Technologies, USA) supplemented with 10% FBS (Gibco, Life Technologies, USA), and 100 unit/ml penicillin plus 100 μ g/ml streptomycin. To induce calcification, HVSMCs were treated with calcifying medium (CM) containing 10 mmol/l β -glycerophosphate (Sigma-Aldrich, USA) and 3 mmol/l calcium chloride (Sigma-Aldrich, USA) [43,44]. In some experiments, Nicotinamide (NAM, Med Chem Express, 5 mM) or AV-153 (Med Chem Express, 100 μ M) was used to treat cells in CM [36,45].

Primary mouse vascular smooth muscle cells (MVSMCs) were isolated from WT mice and CKO mice (6–8 weeks old). Briefly, mice were intraperitoneally euthanized with sodium pentobarbital (150 mg/kg), and thoracic aortas were isolated and cut into small pieces. Then aortic explants were grown in DMEM (Gibco, Life Technologies, USA) containing 10% FBS (Gibco, Life Technologies, USA), 100 unit/ml penicillin plus 100 μ g/ml streptomycin at 37 °C in a humidified incubator. MVSMCs were migrated from aortic explants and cells between passages 3 and 5 were used in this study. MVSMCs were incubated with GM or CM for 5 days.

2.4. Adenovirus infection

Adenovirus encoding SIRT6 (Ad/SIRT6) used in this study were obtained from Vigene Biosciences company (Shandong, China). Ad/GFP was used as negative controls. HVSMCs were seeded in 35 mm dishes and cultured in GM. When the cells reached 80% confluence, Ad/SIRT6 or Ad/GFP at an optimal multiplicity of infection (MOI = 25) was used to transfect cells. SIRT6 expression in cells transfected with Ad/SIRT6 was analyzed by western blot.

2.5. Small interfering RNA (siRNA) transfection

The siRNA used in this study was purchased from Ribobio Co. Ltd. (Guangzhou, China). HVSMCs were seeded at a density of 2×10^5 cells in 35 mm dishes and transfected with SIRT6 siRNA (15 nM, si-SIRT6) or ATM siRNA (15 nM, si-ATM) or scrambled siRNA (si-CTR) by use of Lipofectamine 3000 Transfection Reagent (Thermo Fisher, USA) according to the manufacturer's instructions. The expression of SIRT6 and ATM in cells transfected with siRNA were examined by western blot.

2.6. Arterial ring organ culture

Whole aortas were isolated from 8-week C57BL/6 J mice euthanized by intraperitoneal injection of sodium pentobarbital (150 mg/kg). Human arteries were obtained from patients who underwent the amputation and written informed consent was provided by all patients. Human tissue use was approved by the Ethics Committee of Zhujiang hospital, Southern Medical University, China (Approval number: 2021-KY-079-02) and complied with the Declaration of Helsinki. The characteristics of patients used in this study are included in Supplementary Table 1. Mouse and human arteries were cut into 2–3 mm in length and cultured in GM in a 37 °C incubator with 5% CO₂. Then CM was used to induce calcification of arterial rings for 7 days [8,9,43] after transfection with Ad/SIRT6 or Ad/GFP.

2.7. Alizarin red staining

As described in our previous studies [8,43], alizarin red staining was used to determine calcification in cells and arteries. For cells staining, HVSMCs were seeded in 35 mm dishes. At the indicated time points, HVSMCs were fixed in 4% paraformaldehyde (PFA) for 10 min and stained with 2% alizarin red solution (pH 4.2, Solarbio, Beijing, China) for 5 min at room temperature. Excess dye was removed with deionized water and images were captured by an inverted microscope (Leica, DMi8, Germany). To quantify the extent of calcification, alizarin red dye was eluted with 10% formic acid, the absorbance was measured at 405 nm using a microplate reader (Thermo, NY, USA) and the readings were normalized with control. For tissue staining, the arterial rings were fixed in 10% formalin solution and embedded in paraffin. The arterial samples were cut into 4 μm in thickness on a microtome (Leica, HistoCore MULTICUT, Germany) and then the sections were stained with 2% alizarin red solution for 5 min. Images were captured under an inverted microscope (Leica, DMi8, Germany) and positive red staining areas of aortic rings were analyzed with Image J. For the whole mount of aorta staining, aortic arteries were fixed in 95% ethanol for 24 h and then stained with 0.003% alizarin red solution in 1% potassium hydroxide overnight. The aortas were then washed twice with 2% potassium hydroxide before being photographed.

2.8. Calcium content assay

Calcium content was determined using a Calcium Assay Kit (Leagene Biotechnology, Beijing, China) in accordance with the manufacturer's protocol. Briefly, cells or tissues were centrifuged to separate the supernatant. Then 2.5 μl of samples were mixed with 200 μl of Methyl thymol blue (MTB) solution and incubated for 10 min at room

temperature. The absorbance was measured at 610 nm using a microplate reader (Thermo, NY, USA) and the readings were normalized with control. The protein concentration was measured using the Pierce™ BCA Protein Assay Kit (Thermo Fisher, USA), and calcium content was expressed as μg/mg protein.

2.9. Alkaline phosphatase (ALP) activity assay

ALP activity was assessed using an ALP assay kit (Beyotime, Shanghai, China) according to the manufacturer's guidelines. Mouse arteries were homogenized and the supernatant was separated by centrifugation. The samples were mixed with *p*-nitrophenyl phosphate (*p*-NPP) substrate and incubated for 10 min at 37 °C. The reaction was terminated with 3 mol/l NaOH and the absorbance was measured at 405 nm using a microplate reader (Thermo, NY, USA). Then the results were normalized to the protein levels and ALP activity was calculated as unit/mg protein.

2.10. Comet assay

The alkaline comet assay was performed using a Comet Assay kit (Trevigen, #4250–050-K, Gaithersburg, MD) according to manufacturer's protocol. Briefly, HVSMCs were harvested, centrifuged and suspended in low-temperature-melting agarose gels on comet slides at the indicated time points. The slides were incubated at 4 °C for 30 min to allow the agarose to set and subjected to alkaline electrophoresis in ice electrophoresis solution at 300 mA for 30 min. Then the slides were washed and stained with SYBR Gold (Thermo Fisher, #S11494) for 30 min at room temperature. After being stained, slides were dried completely for 1 h at 37 °C and observed by fluorescent microscope (Leica, DMi8, Germany). The percentage of DNA in the tail and the tail moment were quantified using the Image J plugin OpenComet (<http://cometbio.org/>).

2.11. Immunofluorescence staining

Human arteries, mouse aortas and cultured HVSMCs were harvested at the indicated time points. The characteristics of patients used in this study were listed in Supplementary Table 2. For cell staining, HVSMCs were fixed in 4% PFA and permeabilized by 0.5% Triton X-100 for 15 min at room temperature. Cells were blocked with QuickBlock™ Blocking Buffer for Immunol Staining (Beyotime, Shanghai, China) for 10 min at room temperature, then incubated with primary antibodies diluted in Immunol Staining Primary Antibody Dilution Solution (Beyotime, Shanghai, China) at 4 °C in a humidified chamber overnight. After being washed, cells were incubated with Alexa Fluor secondary antibodies (1:200, Thermo Scientific, USA) for 2 h at room temperature in the dark. Cell nuclei were stained with Hoechst 33342 (Solarbio, Beijing, China), and then captured by a fluorescence microscope (Leica, DMi8, Germany) or a laser scanning confocal microscope (Leica, TCS-SP8, Germany). For tissue staining, the samples were fixed in 10% formalin solution overnight. Fixed tissues were embedded in paraffin and cut into 4 μm in thickness on a microtome (Leica, HistoCore MULTICUT, Germany). The paraffin sections were dewaxed and antigen retrieval was performed by treatment of sections with EDTA Antigen Retrieval Solution (Solarbio, Beijing, China). Then the sections were permeabilized by 0.5% Triton X-100 for 15 min at room temperature, and the other steps were the same as the cell staining. The primary antibodies were used for immunofluorescence staining including anti-SIRT6 (1:200, Abcam, ab62739), anti-γ-H2AX (1:200, Abcam, ab26350), anti-α-SMA (1:200, Abcam, ab7817).

2.12. Western blot analysis

Total protein was extracted from HVSMCs or arterial tissues using RIPA buffer (Thermo Fisher, USA) containing proteinase and

phosphatase inhibitors (Roche, Basel, Switzerland). The protein concentrations were determined by Pierce™ BCA Protein Assay Kit (Thermo Fisher, USA). Proteins were separated by sodium dodecyl sulfate polyacrylamide gel electrophoresis (SDS-PAGE) and then transferred to a polyvinylidene fluoride membrane (PVDF, Millipore, USA). The membranes were blocked by 5% skim milk for 2 h at room temperature and then incubated at 4 °C overnight with the following primary antibodies: anti-RUNX2 (1:1000, Cell Signaling Technology, 12556S), anti-BMP2 (1:1000, Abcam, ab214821), anti- α -SMA (1:5000, Proteintech, 14,395-1-AP), anti-SIRT6 (1:1000, Cell Signaling Technology, 12486S), anti- γ -H2AX (1:1000, Cell Signaling Technology, 2577S), anti-p-ATM (1:1000, Cell Signaling Technology, 5883 T), anti-ATM (1:1000, Cell Signaling Technology, 2873 T) and anti- β -actin (1:10000, Proteintech, HRP-66009). The membranes were washed three times with TBST and incubated with HRP-conjugated secondary antibodies (1:10000, abcam, ab6721) for 1 h at room temperature. The membranes were washed in TBST for another three times and visualized with an enhanced chemiluminescence kit (Millipore, USA) by the Amersham Imager 500 imaging system (GE, Piscataway, NJ, USA) or the ALLIANCE Q9-MICRO imaging system (UVitec, UK). Protein bands were quantified by Image J and normalized to β -actin expression.

2.13. Quantitative real-time PCR

Total RNA was extracted from HVSMCs using TRIzol reagent (Thermo Fisher, USA), and reverse transcription was performed using PrimeScript RT kit (TaKaRa, Japan) according to the manufacturer's protocol. Quantitative real-time PCR (qPCR) was performed on the 7500 FAST real-time PCR system (Applied Biosystems, Foster City, California, USA) using SYBR Green mixture (Takara, Japan). The primers of polymerase chain reaction are as follows: CHD4 (forward 5'-3'): AGGAGCCTAAATCATCTGCTC, CHD4 (reverse 5'-3'): GGGTCTGACAACTGGCTGA; β -actin (forward 5'-3'): CTCTCCAGCCTTCCTCCT, β -actin (reverse 5'-3'): AGCACTGTGTTGGCGTACAG. Relative gene expression was calculated by the comparative Ct (threshold cycle) method and the results were normalized to β -actin.

2.14. Statistical analysis

All statistical analyses were performed using Prism software (Version 8; GraphPad Software) and results were expressed as mean \pm SEM. Data were analyzed for normality and equal variance using GraphPad software. The difference between the two groups was performed by Student's *t*-tests if data had equal variance. The differences between multiple groups were analyzed by one-way ANOVA followed with Tukey HSD test if data had equal variance and with Tamhane T2 test if data had unequal variance. A value of $P < 0.05$ was considered significant.

3. Results

3.1. Expression of SIRT6 is decreased during vascular calcification

To examine the expression of SIRT6 during vascular calcification, HVSMCs and human arterial rings were cultured in CM for 7 days to induce cell calcification *in vitro* and vascular calcification *ex vivo*. Both western blot analysis and immunofluorescence staining showed that SIRT6 was significantly decreased in CM-treated cells compared to GM-treated cells (Fig. 1A, B). Consistently, we also found that the expression of SIRT6 in human arterial rings was significantly reduced in CM group compared to GM group (Fig. 1C). Then, in order to further examine the expression of SIRT6 in vascular calcification *in vivo*, calcified arteries obtained from patients showed markedly reduced SIRT6 expression, as indicated by immunofluorescence staining (Fig. 1D). In addition, western blot analysis and immunofluorescence staining revealed that SIRT6 was also significantly downregulated in VitD₃-overloaded mice compared to vehicle group (Fig. 1E, F). Altogether, these data indicate

that SIRT6 was downregulated during vascular calcification.

3.2. Knockdown of SIRT6 by siRNA promotes HVSMC calcification

To determine the role of SIRT6 in HVSMC calcification, SIRT6 siRNA (si-SIRT6) was used to transfect HVSMCs. Knockdown of SIRT6 in HVSMCs transfected with si-SIRT6 was validated by western blot analysis (Supplementary Fig. 1A). Alizarin red staining showed that si-SIRT6 promoted mineral deposition of HVSMCs in the presence of CM (Fig. 2A), and this result was further confirmed by quantification analysis of alizarin red staining (Fig. 2B). In addition, calcium content assay showed that knockdown of SIRT6 significantly enhanced calcium content (Fig. 2C). Furthermore, we found that knockdown of SIRT6 promoted the expression of osteogenic differentiation markers in HVSMCs, such as Runx2 and BMP2 (Fig. 2D-F). Collectively, these results suggest that knockdown of SIRT6 accelerates osteogenic differentiation and calcification of HVSMCs.

3.3. Overexpression of SIRT6 attenuates HVSMC calcification

To further verify the effect of SIRT6 on HVSMC calcification, HVSMCs were transfected with adenovirus encoding SIRT6 (Ad/SIRT6) in the presence of CM. As shown in Supplementary Fig. 1B, overexpression of SIRT6 in HVSMCs infected with Ad/SIRT6 was confirmed by western blot analysis. Of note, overexpression of SIRT6 markedly attenuated mineral deposition in HVSMCs under CM condition, as indicated by alizarin red staining and quantification of calcium content (Fig. 2G-I). Moreover, western blot analysis revealed that the expression of Runx2 and BMP2 were decreased in cells infected with Ad/SIRT6 (Fig. 2J-L). Together, these data suggest that SIRT6 overexpression protects HVSMCs against calcification.

3.4. Overexpression of SIRT6 alleviates arterial ring calcification

To further investigate the role of SIRT6 in vascular calcification *ex vivo*, mouse aortic rings and human arterial rings were transfected with Ad/SIRT6 in the presence of CM for 7 days. Consistent with the *in vitro* results, alizarin red staining of mouse aortic rings showed that overexpression of SIRT6 remarkably alleviated vascular calcification (Fig. 3A), and this result was further confirmed by quantification analysis of calcified area (Fig. 3B). Consistently, alizarin red staining of human arterial rings revealed that overexpression of SIRT6 inhibited human arterial calcification (Fig. 3C,E). In addition, quantification of calcium content also indicated that overexpression of SIRT6 significantly decreased calcium content in human arterial rings (Fig. 3D). Altogether, these data suggest that SIRT6 overexpression inhibits arterial calcification *ex vivo*.

3.5. Conditional knockout of SIRT6 aggravates mouse aortic calcification

Next, to explore whether knockout of SIRT6 in VSMCs has an effect on vascular calcification *in vivo*, we bred SIRT6^{fl/fl} (WT) mice with SM22 α -Cre transgenic mice to obtain SIRT6 conditional knockout (CKO) mice. The mouse genotyping was analyzed by polymerase chain reaction (PCR) of genomic DNA (Supplementary Fig. 2). We isolated mouse vascular smooth muscle cells (MVSMCs) from WT mice and CKO mice, knockout of SIRT6 in MVSMCs was confirmed by immunofluorescence staining (Supplementary Fig. 3A). Alizarin red staining shown that mineral deposition was increased in CKO group compared with WT under CM condition (Fig. 4A). Next, knockout of SIRT6 in mouse aortas was validated by western blot analysis (Supplementary Fig. 3B) and immunofluorescence staining (Supplementary Fig. 3C). Alizarin red staining of mouse aortas and aortic sections showed that aortic calcification was aggravated in CKO mice compared with WT mice (Fig. 4B-C). Consistently, quantification analysis of calcium content further confirmed that knockout of SIRT6 increased calcium content in mouse

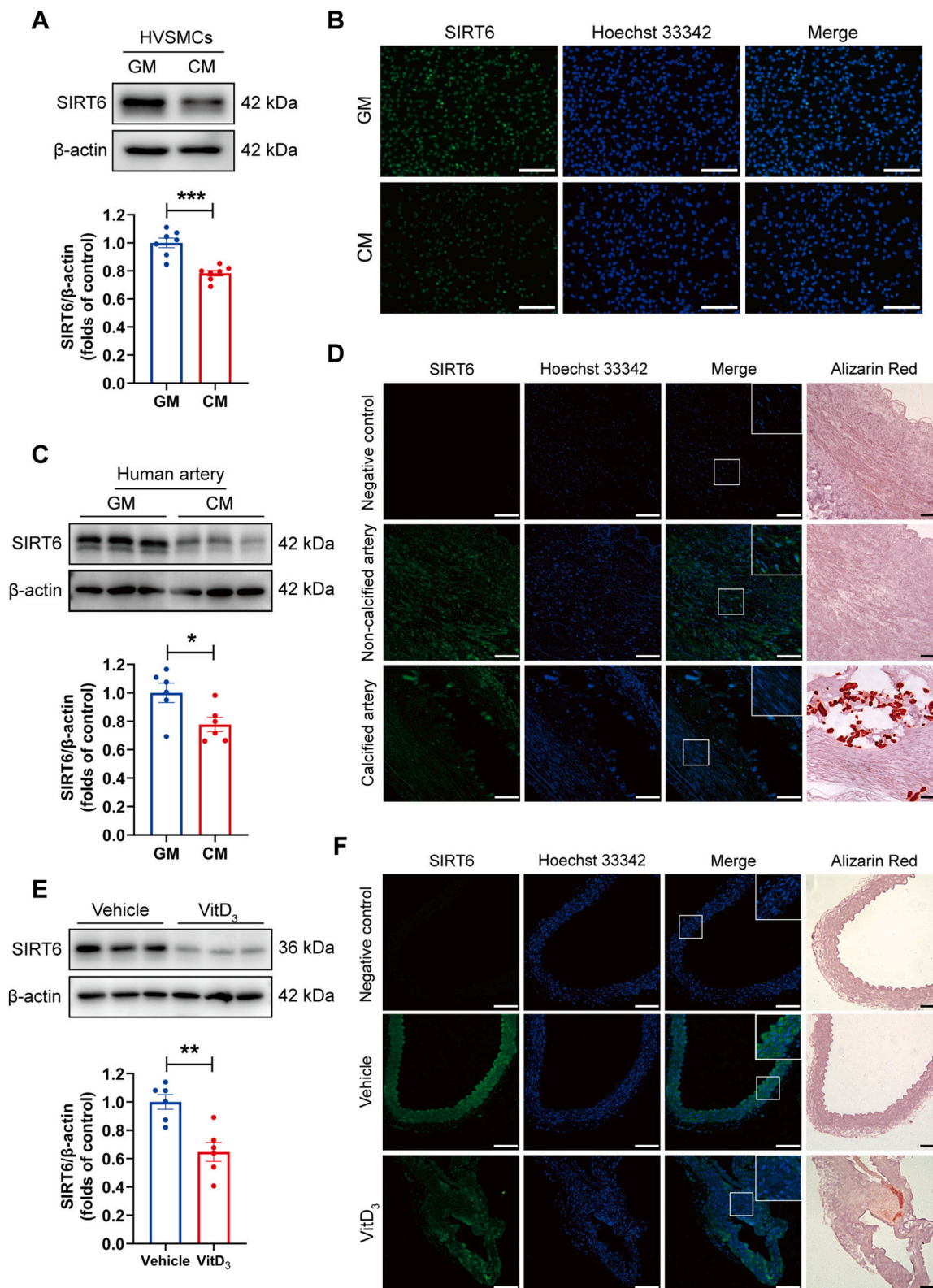
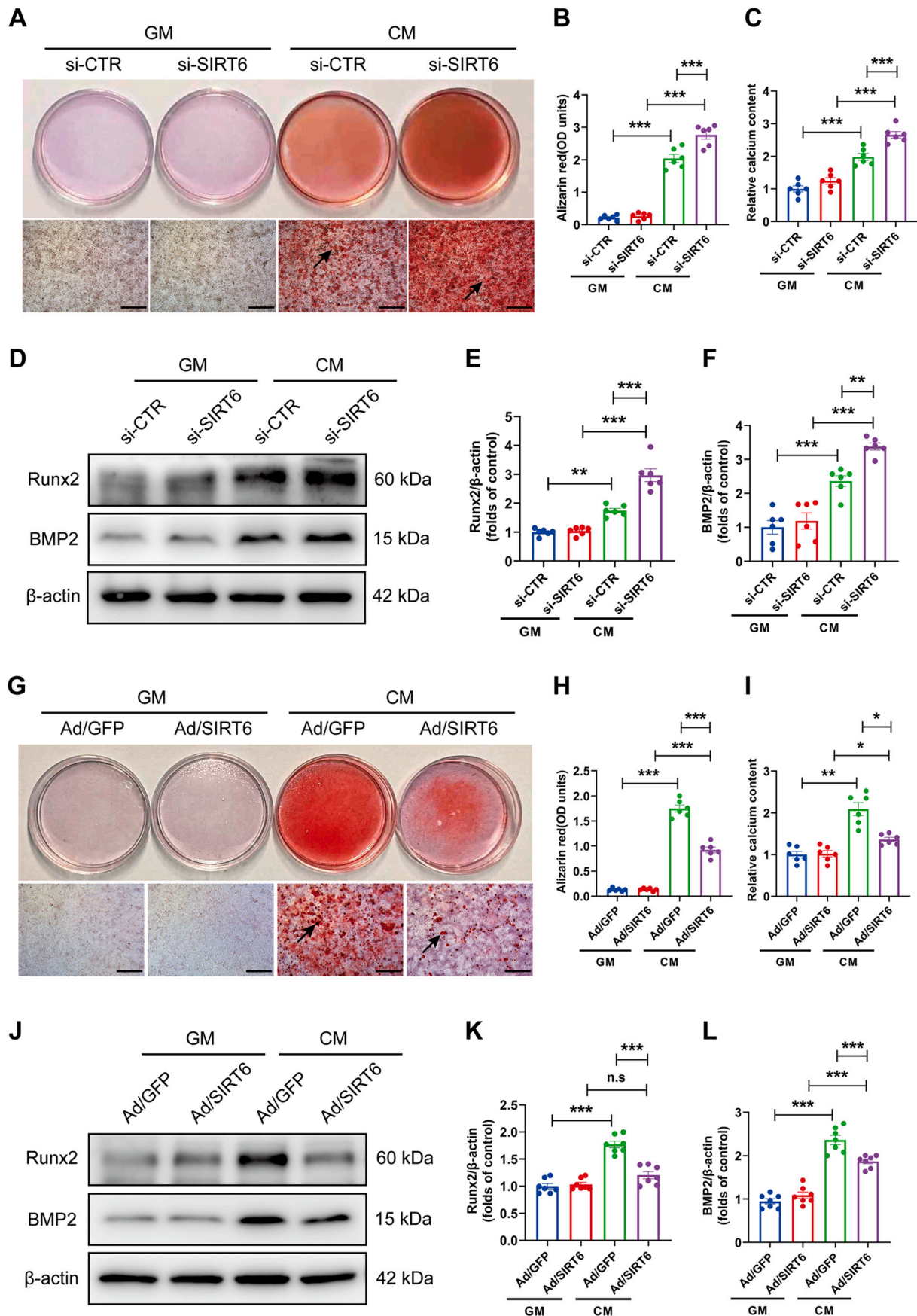


Fig. 1. Expression of SIRT6 is decreased during vascular calcification. Human vascular smooth muscle cells (HVSMCs) and human arterial rings were incubated with growth medium (GM) or calcifying medium (CM) for 7 days (A–C), and aortic calcification of mice was induced by Vitamin D₃ (VitD₃) (E–F). (A–B) Western blot analysis and immunofluorescence staining of SIRT6 expression in HVSMCs (n = 7). Scale bar = 250 μ m. (C) Western blot analysis of SIRT6 expression in human arterial rings (n = 6). (D) Immunofluorescence staining and alizarin red staining of human calcified arteries. Scale bar = 100 μ m. (E) Western blot analysis of SIRT6 expression in aortas of VitD₃-overloaded mice (n = 6). (F) immunofluorescence staining and alizarin red staining of SIRT6 expression in aortas of VitD₃-overloaded mice. Scale bar = 100 μ m. Statistical significance was performed by two-tailed Student *t*-test. **P* < 0.05, ***P* < 0.01, ****P* < 0.001. HVSMCs, human vascular smooth muscle cells; GM, growth medium; CM, calcifying medium; VitD₃, vitamin D₃. (For interpretation of the references to colour in this figure legend, the reader is referred to the web version of this article.)



(caption on next page)

Fig. 2. SIRT6 attenuates human vascular smooth muscle cell calcification. Human vascular smooth muscle cells (HVSMCs) were transfected with si-SIRT6 (A-F) or Ad/SIRT6 (G-L) in growth medium (GM) or calcifying medium (CM) for 7 days. (A&G) Alizarin red staining was used to assess mineral deposition in HVSMCs ($n = 6$). Scale bar = 500 μm . (B&H) Quantitative analysis of alizarin red dye by a microplate reader ($n = 6$). Statistical significance was performed by one-way ANOVA with Tukey HSD test (siRNA group) or Tamhane T2 test (adenovirus group). (C&I) Calcium content in HVSMCs was measured by calcium content assay ($n = 6$). Statistical significance was performed by one-way ANOVA with Tukey HSD test (siRNA group) or Tamhane T2 test (adenovirus group). (D-F&J-L) BMP2 and Runx2 expression was analyzed by western blot and quantified by densitometry ($n = 6-7$). Statistical significance was performed by one-way ANOVA with Tukey HSD test. * $P < 0.05$, ** $P < 0.01$, *** $P < 0.001$ and n.s indicates no significance. Runx2, Runt-related transcription factor 2; BMP2, bone morphogenetic protein 2. (For interpretation of the references to colour in this figure legend, the reader is referred to the web version of this article.)

aortas (Fig. 4D). Moreover, ALP activity, an osteogenic differentiation marker, was remarkably increased after treatment with VitD₃ and further enhanced in CKO mice (Fig. 4E). Additionally, western blot analysis revealed that knockout of SIRT6 downregulated the expression of α -SMA, a smooth muscle marker, but upregulated the expression of BMP2 (Fig. 4F-H). Collectively, these findings indicate that knockout of SIRT6 in VSMCs aggravates aortic calcification in VitD₃-overloaded mice.

3.6. Knockdown of SIRT6 exacerbates DNA damage during HVSMC calcification

Given that DNA damage is involved in the progression of vascular calcification [13,14,22], and SIRT6 can enhance DNA repair to reduce the damage [35,46], we investigated whether loss of SIRT6 promoted vascular calcification involving DNA damage repair. SIRT6 siRNA was used to transfect HVSMCs to knock down SIRT6. A single-cell comet assay was performed to evaluate the extent of DNA DSBs. We found that DNA damage was significantly increased under CM condition compared with GM, and knockdown of SIRT6 exacerbated DNA damage (Fig. 5A-C). In addition, we performed western blot and immunofluorescence staining to analyze the expression of γ -H2AX, a biomarker for DNA DSBs [21,47]. Both the expression of γ -H2AX and the formation of γ -H2AX foci were significantly increased in CM-treated cells compared to GM-treated cells. Moreover, knockdown of SIRT6 elevated the levels of γ -H2AX (Fig. 5D-G). Taken together, these findings suggest that loss of SIRT6 promotes DNA DSBs during HVSMC calcification.

3.7. Overexpression of SIRT6 alleviates DNA damage during HVSMC calcification

Next, to further confirm the role of SIRT6 in DNA damage during HVSMC calcification, Ad/SIRT6 was used to overexpress SIRT6 in HVSMCs. As expected, comet assay showed that overexpression of SIRT6 markedly attenuated DNA damage induced by CM treatment (Fig. 5H-J). Moreover, western blot analysis and immunofluorescence staining revealed that the DSBs marker γ -H2AX was decreased after overexpression of SIRT6 (Fig. 5K-N). Hence, these results indicate that upregulation of SIRT6 alleviates DNA DSBs in the process of HVSMC calcification.

3.8. Enhanced DNA repair reverses HVSMC calcification induced by SIRT6 deficiency

To determine whether DNA damage repair plays an important role during HVSMC calcification in SIRT6 deficiency, we used AV-153, a DNA repair agent, to repair DNA damage [45,48]. Comet assay revealed that DNA damage was significantly aggravated in si-SIRT6, and this effect was alleviated after treatment with AV-153 under CM condition (Supplementary Fig. 4A-C). Alizarin red staining showed that si-SIRT6 promoted HVSMC calcification, and this effect of si-SIRT6 was abolished by AV-153 in the presence of CM (Supplementary Fig. 4D), and this results was further confirmed by quantification of alizarin red staining (Supplementary Fig. 4E).

3.9. SIRT6 attenuates DNA damage independent of its catalytic activity in HVSMC calcification

In order to verify whether SIRT6 alleviates DNA damage relying on its enzyme activity during HVSMC calcification. We used nicotinamide (NAM) to inhibit SIRT6 catalytic activity. Alizarin red staining shown that Ad/SIRT6 attenuated HVSMC calcification, and this effect of Ad/SIRT6 was abolished by NAM in the presence of CM (Fig. 6A). These results were further confirmed by quantification of alizarin red staining that mineral deposition (Fig. 6B). However, we found that overexpression SIRT6 significantly alleviated DNA damage, as showed by comet assay and γ -H2AX foci, whereas NAM treatment had no significant effect on DNA damage compared with Ad/SIRT6 (Fig. 6C-G).

3.10. ATM signal is required for the inhibitory role of SIRT6 in HVSMC calcification

Since ATM as a critical mediator is mainly activated by DSBs [49] and SIRT6 has been proven to be a sensor that can directly recognize DSBs and recruit proteins of DDR, including ATM [36], we investigated whether SIRT6 also regulated the expression of ATM under CM conditions. HVSMCs were treated with siSIRT6 or Ad/SIRT6 under CM conditions. Consistent with previous studies [50], our results also showed that knockdown of SIRT6 decreased the expression of p-ATM (Fig. 7A-B), but not ATM (Supplementary Fig. 5A), whereas overexpression of SIRT6 increased p-ATM expression (Fig. 7C-D), but not ATM (Supplementary Fig. 5B), suggesting that SIRT6 positively regulates p-ATM expression.

Next, we wondered whether SIRT6 relies on ATM to initiate DDR and promote DNA repair to reduce vascular calcification. Knockdown of ATM in HVSMCs transfected with siATM was validated by western blot analysis (Supplementary Fig. 6). Alizarin red staining revealed that Ad/SIRT6 attenuated HVSMC calcification, and this effect of Ad/SIRT6 was antagonized by knockdown of ATM in the presence of CM (Fig. 7E). These results were further confirmed by quantification of alizarin red staining (Fig. 7F). Moreover, calcium content assay showed that overexpression of SIRT6 significantly alleviated mineral deposition, and knockdown of ATM abolished the reduction of mineral deposition under CM conditions (Fig. 7G). Furthermore, we found that Ad/SIRT6 decreased the expression of osteogenic differentiation markers, such as Runx2 and BMP2, and the inhibitory effect on Runx2 and BMP2 expression was abrogated by si-ATM in the presence of CM (Fig. 7H-J). In addition, we found that SIRT6 overexpression significantly alleviated DNA DSBs, as indicated by comet assay and γ -H2AX foci, and the protective effect of SIRT6 overexpression against DNA DSBs was abolished by knockdown of ATM (Fig. 7K-O). Altogether, these data indicate that SIRT6 repairs DNA DSBs and inhibits vascular calcification relying on activation of ATM.

3.11. SIRT6 activates ATM via CHD4 in HVSMC calcification

It has been reported that a necessary condition for DNA repair is chromatin relaxation which induces ATM activated [17,51]. Chromatin helicase DNA binding protein 4 (CHD4), a chromatin relaxation factor, plays a role in DNA damage response [52]. To determine whether SIRT6 activates ATM through CHD4, CHD4 siRNA (si-CHD4) and Ad/SIRT6 were used to transfect HVSMCs under CM conditions. Knockdown of

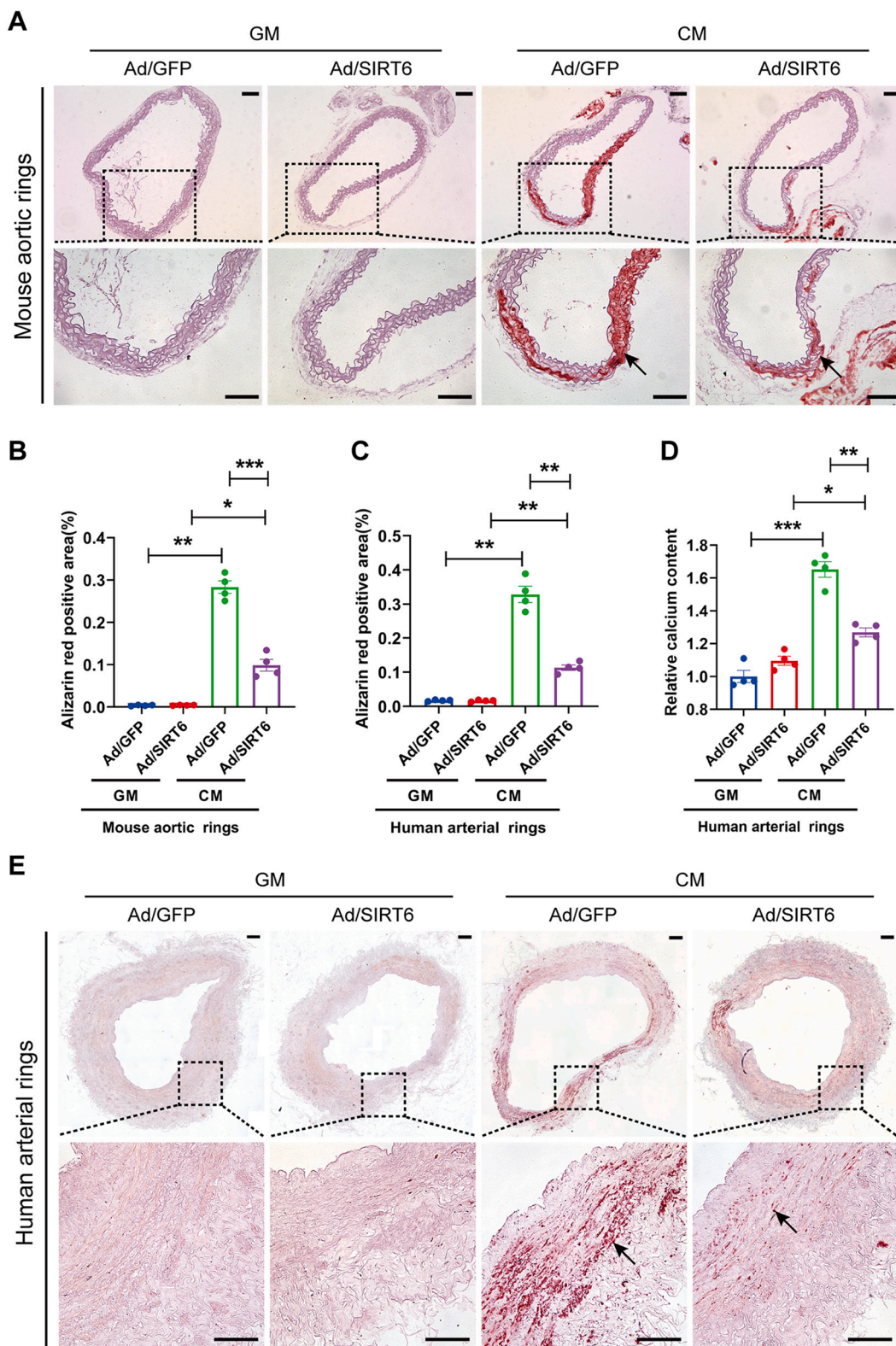


Fig. 3. Overexpression of SIRT6 alleviates arterial ring calcification. Mouse aortic rings and human arterial rings were transfected with Ad/GFP or Ad/SIRT6 in growth medium (GM) or calcifying medium (CM) for 7 days (n = 4). (A&E) Mineral deposition in mice aortic rings (A) and human arterial rings (E) was detected by alizarin red staining. Scale bar = 100 μ m (mouse aortic rings) and 250 μ m (human arterial rings). (B-C) Positive area of alizarin red staining in mouse aortic rings and human arterial rings was quantified by Image J. (D) Calcium content in human arterial rings was measured by calcium content assay. Statistical significance was performed by one-way ANOVA with Tamhane T2 test. * $P < 0.05$, ** $P < 0.01$, *** $P < 0.001$. (For interpretation of the references to colour in this figure legend, the reader is referred to the web version of this article.)

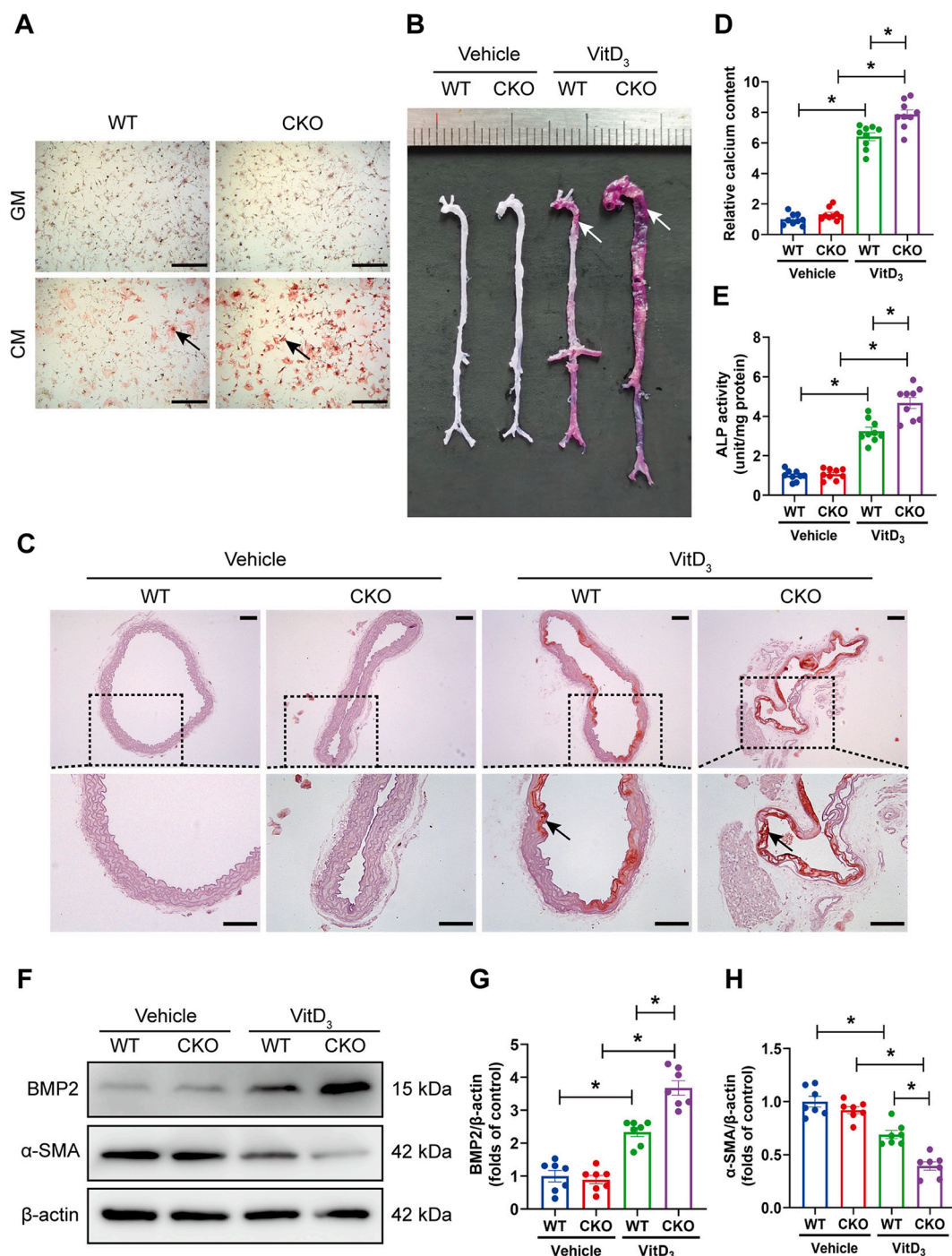


Fig. 4. Smooth muscle cell-specific knockout of SIRT6 promotes calcification in mouse vascular smooth muscle cells and Vitamin D₃-overloaded mouse aortas. Mouse vascular smooth muscle cells (MVSMCs) were incubated with growth medium (GM) or calcifying medium (CM) for 5 days and mouse aortic calcification model was induced by subcutaneous injection with Vitamin D₃ (VitD₃, 5×10^5 IU/kg) for consecutive 3 days and then fed for another 6 days. (A) Alizarin red staining was used to assess mineral deposition in MVSMCs. Scale bar = 500 μ m. (B) Mouse aortic calcification was detected by alizarin red staining (n = 6–8). (C) Calcification of mouse aortic sections was detected by alizarin red staining. Scale bar = 100 μ m. (D) Calcium content in mouse aortas was measured (n = 9). (E) Quantification of ALP activity in mouse aortas (n = 9). (F–H) BMP2 and α -SMA expression was analyzed by western blot and quantified by densitometry (n = 7). Statistical significance was performed by one-way ANOVA with Tukey HSD test. * $P < 0.001$. WT, wild type; CKO, conditional knockout; ALP, alkaline phosphatase; α -SMA, alpha smooth muscle actin. (For interpretation of the references to colour in this figure legend, the reader is referred to the web version of this article.)

CHD4 in HVSMCs transfected with si-CHD4 was validated by qPCR analysis (Fig. 8A). Then western blot results showed that overexpression of SIRT6 increased the expression of p-ATM, while knockdown of CHD4 abrogated the upregulated of p-ATM in the presence of CM, and ATM expression remained unchanged (Fig. 8B–D). Alizarin red staining

revealed that Ad/SIRT6 attenuated HVSMC calcification, and this effect of Ad/SIRT6 was partly abolished by knockdown of CHD4 under CM conditions (Fig. 8E). These results were further confirmed by quantification of alizarin red staining (Fig. 8F).

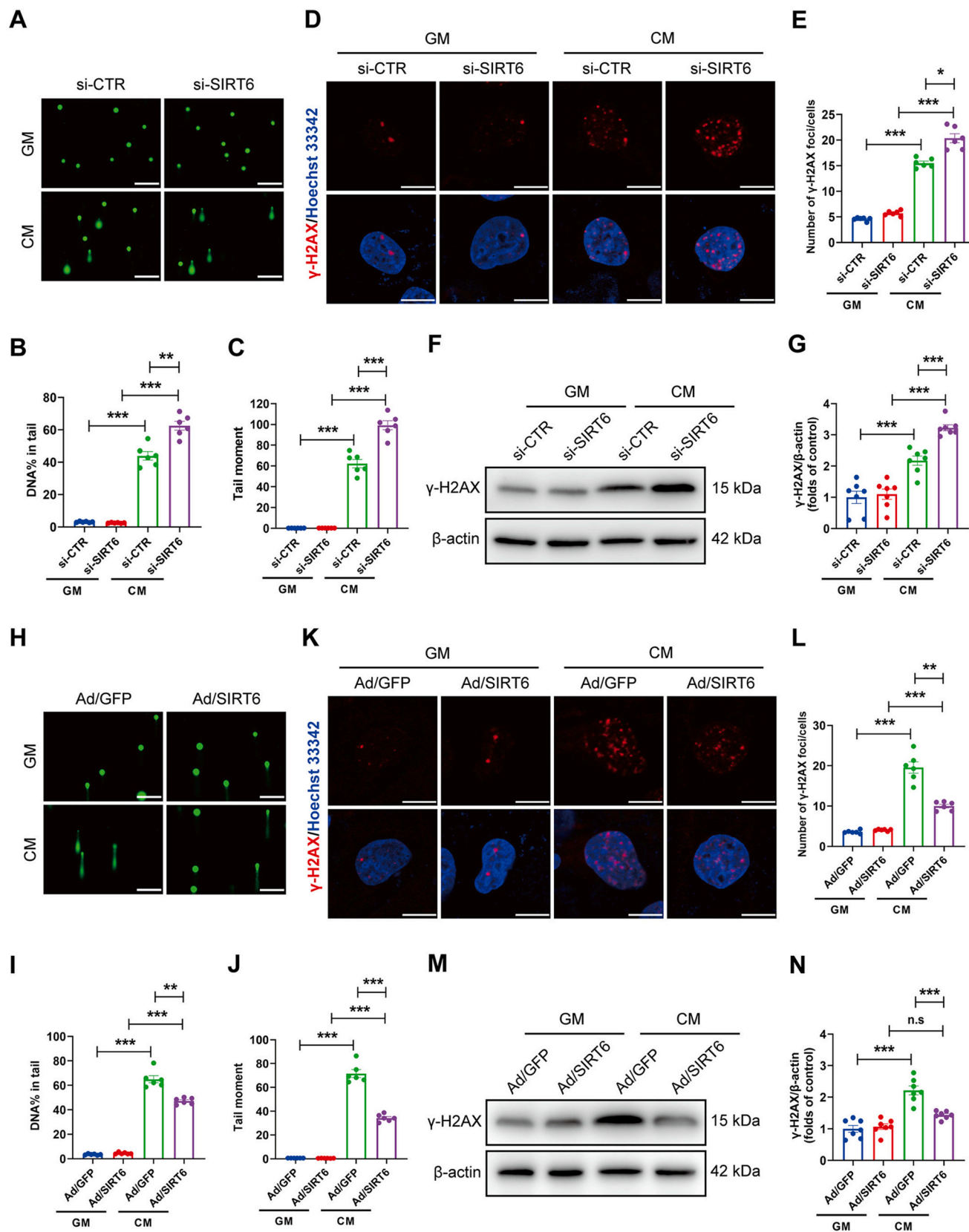


Fig. 5. SIRT6 attenuates DNA damage during human vascular smooth muscle cell calcification. Human vascular smooth muscle cells (HVSMSCs) were transfected with si-SIRT6 (A-G) or Ad/SIRT6 (H-N) in growth medium (GM) or calcifying medium (CM) for 7 days. (A-C&H-J) Representative comet assay and analysis of tail DNA percentage, and tail moment were calculated via Image J plugin OpenComet (n = 6). Scale bar = 250 μm. Statistical significance was performed by one-way ANOVA with Tamhane T2 test. (D-E&K-L) immunofluorescence staining of γ-H2AX expression (n = 6). Scale bar = 10 μm. Statistical significance was performed by one-way ANOVA with Tamhane T2 test. (F-G&M-N) Western blot analysis of phosphorylation of histone H2AX on serine 139 (γ-H2AX) expression (n = 7). Statistical significance was performed by one-way ANOVA with Tukey HSD test. **P* < 0.05, ***P* < 0.01, ****P* < 0.001 and n.s indicates no significance.

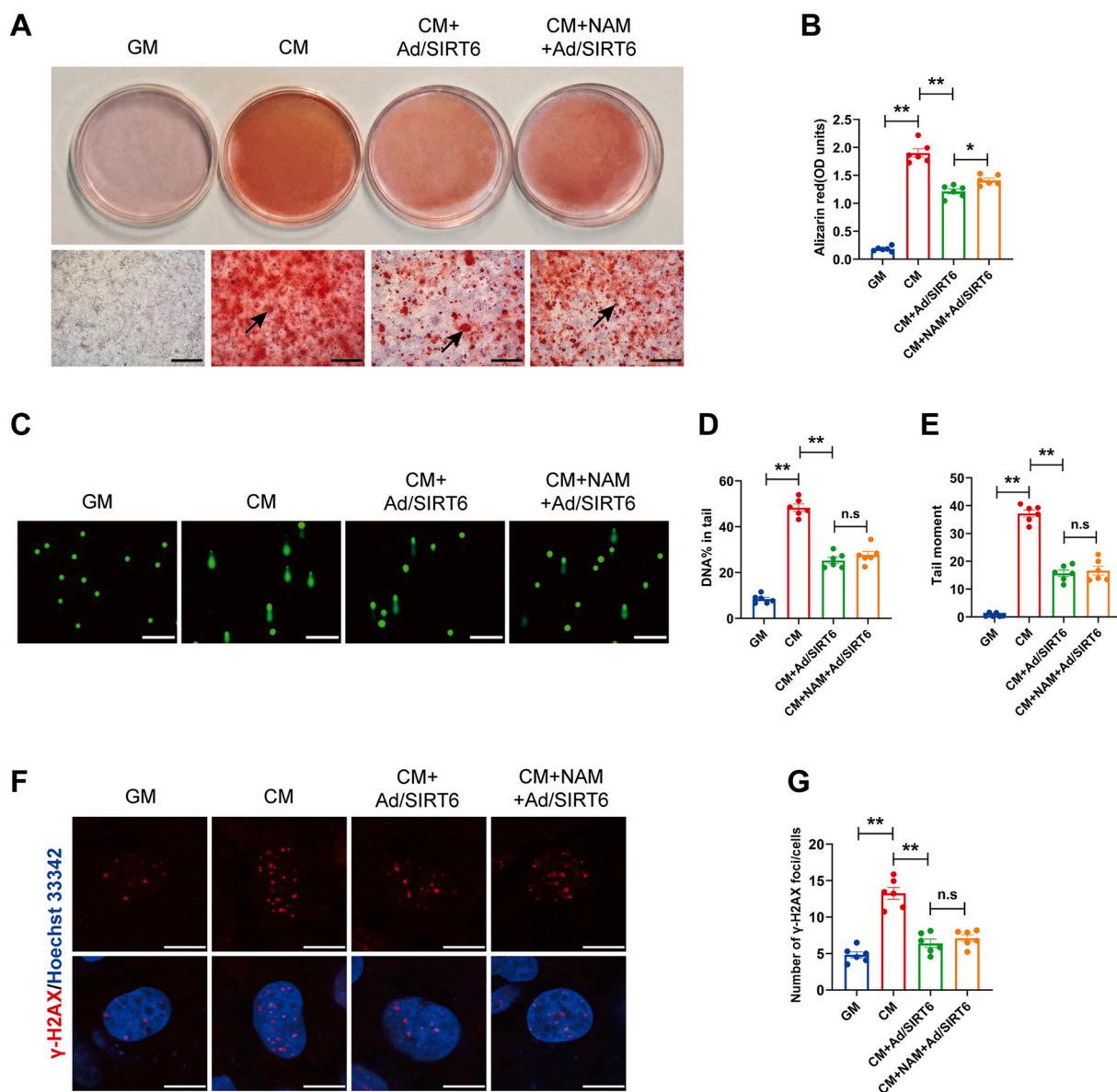


Fig. 6. SIRT6 attenuates DNA damage independent of its catalytic activity during HVSMC calcification. Human vascular smooth muscle cells (HVSMCs) were transfected with Ad/SIRT6 and treated with nicotinamide (NAM) in calcifying medium (CM) for 7 days ($n = 6$). (A) Alizarin red staining was used to assess mineral deposition in HVSMCs. Scale bar = 500 μm . (B) Quantitative analysis of alizarin red dye by a microplate reader. (C–E) Representative comet assay and analysis of tail DNA percentage, and tail moment were calculated via Image J plugin OpenComet. Scale bar = 250 μm . (F–G) Immunofluorescence staining of γ -H2AX expression. Scale bar = 10 μm . Statistical significance was performed by one-way ANOVA with Tukey HSD test. $*P < 0.05$, $**P < 0.001$ and n.s. indicates no significance. (For interpretation of the references to colour in this figure legend, the reader is referred to the web version of this article.)

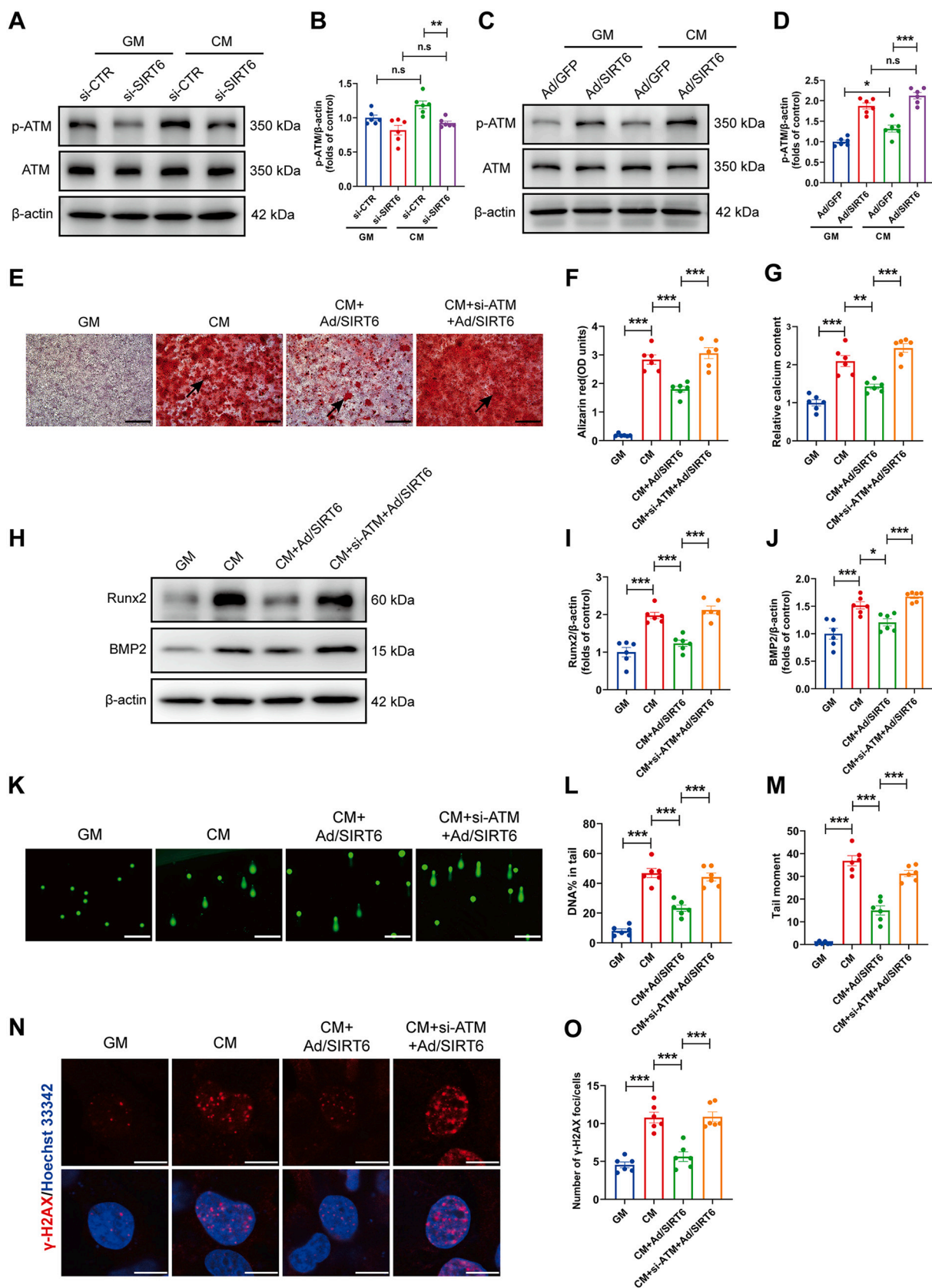
4. Discussion

In this study, we for the first time demonstrated that specific deletion of SIRT6 in VSMCs contributes to vascular calcification via suppression of DNA damage repair. Firstly, we found that the expression of SIRT6 is decreased during calcification in HVSMCs, arterial rings, aortas of VitD_3 -overloaded mice and human arteries. Next, we found that knockdown of SIRT6 aggravates HVSMC calcification and DNA damage, and overexpression of SIRT6 shows the opposite effects. Moreover, *ex vivo* experiments confirmed that overexpression of SIRT6 inhibits the calcification of mouse and human arterial rings. Furthermore, *in vivo* experiments showed smooth muscle cell-specific knockout of SIRT6 significantly aggravates aortic calcification in VitD_3 -overloaded mice. Additionally, we found that knockdown of ATM counteracted the protective effect of SIRT6 on HVSMC calcification and DNA damage.

SIRT6 has beneficial effects on lifespan-extending and anti-aging

[37]. Previous studies reported that SIRT6 plays a protective effect on VSMCs by inhibiting senescence and reducing atherogenesis [34]. SIRT6 is crucial for maintaining the contractile phenotype of VSMCs under cyclic strain [53]. Moreover, a recent study has reported that exosomes, derived from bone marrow mesenchymal stem cell, inhibit mouse aortic calcification via SIRT6–HMGB1 deacetylation pathway in chronic kidney disease model [54]. In our study, we for the first time demonstrated that conditional knockout of SIRT6 in VSMCs exacerbates aortic calcification in VitD_3 -overloaded mice. Similarly, a latest study has shown that vascular calcification was reduced via the SIRT6–Runx2 pathway in chronic kidney disease model using SIRT6-transgenic mice [55]. Taken together, these findings indicate that loss of SIRT6 in VSMCs promotes vascular calcification.

It has been reported that persistent DNA damage and impaired DNA damage repair exist in VSMCs under osteogenic conditions [22,23]. A recent study has revealed that there is a link between the osteogenic



(caption on next page)

Fig. 7. Knockdown of ATM abolishes the inhibitory effect of SIRT6 overexpression on calcification and DNA damage during human vascular smooth muscle cell calcification. Human vascular smooth muscle cells (HVSMCs) were transfected with Ad/SIRT6 (A-B) or siSIRT6 (C-D) under CM conditions in growth medium (GM) or calcifying medium (CM), and transfected with Ad/SIRT6 and si-ATM (E-O) in the presence of calcifying medium (CM) for 7 days (n = 6). (A-D) Western blot analysis of p-ATM expression. (E) Alizarin red staining was used to assess HVSMC calcification. Scale bar = 500 μ m. (F) Quantitative analysis of alizarin red dye by a microplate reader. Statistical significance was performed by one-way ANOVA with Tukey HSD test. (G) Calcium content was measured by calcium content assay. Statistical significance was performed by one-way ANOVA with Tukey HSD test. (H-J) BMP2 and Runx2 expression was analyzed by western blot and quantified by densitometry. Statistical significance was performed by one-way ANOVA with Tukey HSD test. (K-M) Representative comet assay and analysis of tail DNA percentage, and tail moment were calculated via Image J plugin OpenComet. Scale bar = 250 μ m. Statistical significance was performed by one-way ANOVA with Tukey HSD test (tail DNA percentage) and with Tamhane T2 test (tail moment). (N-O) Immunofluorescence staining of phosphorylation of histone H2AX on serine 139 (γ -H2AX) expression. Scale bar = 10 μ m. Statistical significance was performed by one-way ANOVA with Tukey HSD test. * P < 0.05, ** P < 0.01, *** P < 0.001 and n.s indicates no significance. ATM, ataxia telangiectasia mutation; p-ATM, phosphorylation of ataxia telangiectasia mutation at Ser1981; γ -H2AX, phosphorylation of histone H2AX on serine 139. (For interpretation of the references to colour in this figure legend, the reader is referred to the web version of this article.)

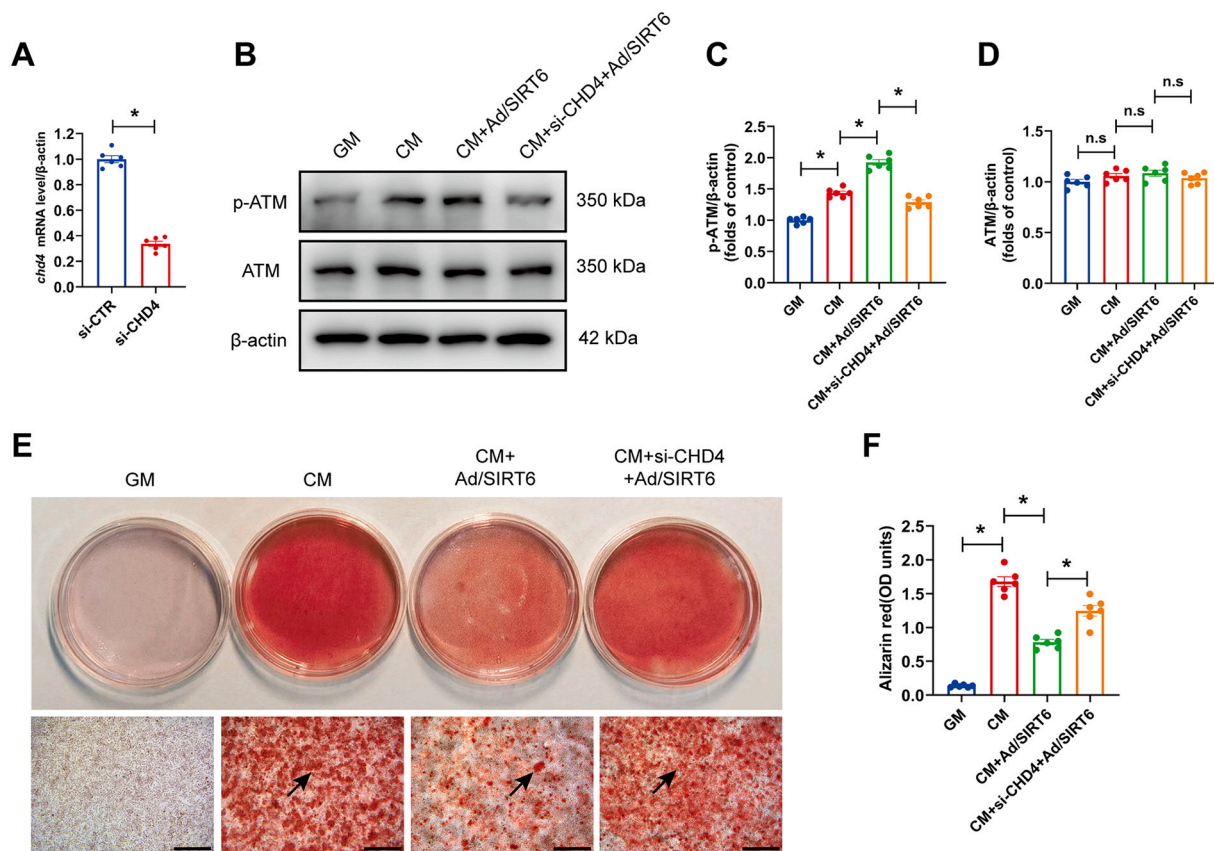


Fig. 8. SIRT6 activates ATM via CHD4 in HVSMC calcification. Human vascular smooth muscle cells (HVSMCs) were transfected with Ad/SIRT6 and si-CHD4 in the presence of calcifying medium (CM) for 7 days (n = 6). (A) Quantitative real-time PCR analysis of CHD4 expression. Statistical significance was performed by two-tailed Student *t*-test. (B-D) Western blot analysis of the expression of p-ATM and ATM. (E) Alizarin red staining was used to assess HVSMC calcification. Scale bar = 500 μ m. (F) Quantitative analysis of alizarin red dye by a microplate reader. Statistical significance was performed by one-way ANOVA with Tukey HSD test. * P < 0.001 and n.s indicates no significance. (For interpretation of the references to colour in this figure legend, the reader is referred to the web version of this article.)

protein RUNX2 and DNA damage, and DNA damage enhances vascular calcification in a RUNX2-dependent manner under the high phosphorus and calcium condition [13]. However, inhibition of ROS-induced DNA damage reduces calcification of MVSMCs induced by high glucose [56,57], and another study showed that restoring sirtuin1 (SIRT1) level initiates DDR, thus repairing damaged DNA and preventing senescence in diabetic vascular calcification [14]. These results indicated that DNA damage exists in vascular calcification and inhibiting or repairing damaged DNA reduces vascular calcification. In addition, previous studies have shown that SIRT6 maintains genomic stability by reducing DNA damage and promoting DDR. For example, SIRT6 alleviates DNA damage via enhancing telomerase activity in hypertrophic ligamentum flavum cells [33], and reduces DNA damage induced by doxorubicin via initiating DDR in osteosarcoma [50]. In endothelial cells, SIRT6 protects

from telomere dysfunction and DNA damage, thus preventing senescence [58]. It is worth noting that SIRT6 also reduces DNA damage of VSMC senescence in atherosclerosis by maintaining the integrity of telomeres [34]. In this study, We found that DNA DSBs was attenuated by overexpression of SIRT6, and aggravated by knockdown of SIRT6 during VSMC calcification. Enhancing DNA repair alleviated VSMC calcification induced by SIRT6 knockdown. We for the first time pointed out that SIRT6 deficiency in VSMCs mediates vascular calcification involving DNA damage. Previous studies have reported that SIRT6 overexpression inhibits vascular calcification in chronic kidney disease mice through its deacetylation activity [55]. However, in our study, we have demonstrated that SIRT6 prevents vascular calcification by attenuating DNA damage, not just deacetylation effects.

DDR is a signaling cascade process in response to DNA damage, in

which ATM as a key mediator is mainly activated by DSBs, thus activating downstream effector proteins [49]. A recent study has reported that SIRT1 activation promotes the formation of DDR sensor and upregulates ATM to reduce DNA damage in diabetic vascular calcification [14]. Similarly, SIRT6 reduces doxorubicin induced-DNA damage by activating the ATM pathway in osteosarcoma [50]. Consistently, we found that SIRT6 overexpression reduces DNA damage by upregulating p-ATM during VSMC calcification. During the process of DDR, ATM is activated just as a mediator and whether the sensors, upstream of the mediators, can correctly identify the damaged DNA is considered to be more critical. Recent studies reported that SIRT6 acts as an independent sensor to identify DSBs during DDR [35,36]. We speculate that SIRT6 acts as a sensor to recognize DSBs and activate DDR via upregulating p-ATM during vascular calcification. Previous studies have reported that chromatin relaxation is a prerequisite for DDR, and ATM is activated in response to change in chromatin conformation after DSBs rather than direct contact with broken DNA [17,51]. This may explain the increased activation of ATM during vascular calcification. CHD4 is a chromatin relaxation factor which is closely related to DDR [52,59]. Previous studies have reported that SIRT6 rapidly arrives at DNA damage sites and recruits CHD4 to promote chromatin relaxation and DNA repair, which are associated with ATM [46]. In this study, we found that SIRT6 overexpression increased p-ATM via CHD4 during VSMC calcification. Collectively, SIRT6 deficiency in VSMCs leads to aggravation of vascular calcification by exacerbating DNA damage, and SIRT6 activation alleviates DNA damage and HSMC calcification via upregulating p-ATM.

The limitation of this study is that SIRT6 has multiple biological functions including anti-inflammatory, anti-oxidative stress and anti-aging [34], but we only investigated the effect of SIRT6 on DNA DSBs. In addition, flow condition may affect vascular calcification, but our *in vitro* and *ex vivo* experiments has been carried out in the medium without hemodynamic stimuli.

In conclusion, this study demonstrated that the loss of SIRT6 in VSMCs exacerbates vascular calcification at least partly by suppressing DNA damage repair and SIRT6 promotes ATM activation, leading to decreased DNA damage during vascular calcification. This provides new insights into the role of SIRT6 in vascular calcification and the development of SIRT6 analogs may represent a novel strategy for the treatment of vascular calcification.

Author contributions

S. Wang performed experiments, analyzed the data and wrote the draft. L. Li and Q. Liang, performed experiments and analyzed the data. Y. Ye, Z. Lan, Q. Dong, A. Chen, M. Fu, Y. Li, X. Liu, and JS. Ou performed experiments. L. Lu conceived and designed the experiments. J. Yan conceived and designed the experiments, analyzed the data, and revised the manuscript.

Funding

This work was supported by the National Natural Science Foundation of China (82070246, 81870190, 82170414, and 81830013); National Key R&D Program of China (2021YFA0805100), and Guangdong Basic and Applied Basic Research Foundation (2021A1515010752, 2019A1515010682, and 2021A1515011044).

Declaration of Competing Interest

The authors have declared no competing interests.

Acknowledgments

None.

Appendix A. Supplementary data

Supplementary data to this article can be found online at <https://doi.org/10.1016/j.jmcc.2022.10.009>.

References

- [1] M.A. Rogers, E. Aikawa, Cardiovascular calcification: artificial intelligence and big data accelerate mechanistic discovery, *Nat. Rev. Cardiol.* 16 (5) (2019) 261–274.
- [2] A.L. Durham, M.Y. Speer, M. Scatena, C.M. Giachelli, C.M. Shanahan, Role of smooth muscle cells in vascular calcification: implications in atherosclerosis and arterial stiffness, *Cardiovasc. Res.* 114 (4) (2018) 590–600.
- [3] P. Lanzer, M. Boehm, V. Sorribas, M. Thiriet, J. Janzen, T. Zeller, H.C. St. C. Shanahan, Medial vascular calcification revisited: review and perspectives, *Eur. Heart J.* 35 (23) (2014) 1515–1525.
- [4] Y. Chen, X. Zhao, H. Wu, Arterial stiffness: a focus on vascular calcification and its link to bone mineralization, *Arterioscler. Thromb. Vasc. Biol.* 40 (5) (2020) 1078–1093.
- [5] D. Proudfoot, Calcium signaling and tissue calcification, *Cold Spring Harb. Perspect. Biol.* 11 (10) (2019), a35303.
- [6] V.P. Iyemere, D. Proudfoot, P.L. Weissberg, C.M. Shanahan, Vascular smooth muscle cell phenotypic plasticity and the regulation of vascular calcification, *J. Intern. Med.* 260 (3) (2006) 192–210.
- [7] Y. Sun, C.H. Byon, K. Yuan, J. Chen, X. Mao, J.M. Heath, A. Javed, K. Zhang, P. G. Anderson, Y. Chen, Smooth muscle cell-specific runx2 deficiency inhibits vascular calcification, *Circ. Res.* 111 (5) (2012) 543–552.
- [8] X. Liu, A. Chen, Q. Liang, X. Yang, Q. Dong, M. Fu, S. Wang, Y. Li, Y. Ye, Z. Lan, Y. Chen, J.S. Ou, P. Yang, L. Lu, J. Yan, Spermidine inhibits vascular calcification in chronic kidney disease through modulation of SIRT1 signaling pathway, *Aging Cell* 20 (6) (2021), e13377.
- [9] X. Zhang, Y. Li, P. Yang, X. Liu, L. Lu, Y. Chen, X. Zhong, Z. Li, H. Liu, C. Ou, J. Yan, M. Chen, Trimethylamine-N-oxide promotes vascular calcification through activation of NLRP3 (nucleotide-binding domain, leucine-rich-containing family, pyrin domain-containing-3) inflammasome and NF- κ B (nuclear factor κ B) signals, *Arterioscler. Thromb. Vasc. Biol.* 40 (3) (2020) 751–765.
- [10] T. Chen, C. Lin, S. Chien, S. Chang, C. Chen, Regulation of calcification in human aortic smooth muscle cells infected with high-glucose-treated *Porphyromonas gingivalis*, *J. Cell. Physiol.* 233 (6) (2018) 4759–4769.
- [11] L.A. Pescatore, L.F. Gamarra, M. Liberman, Multifaceted mechanisms of vascular calcification in aging, *Arterioscler. Thromb. Vasc. Biol.* 39 (7) (2019) 1307–1316.
- [12] P. Bautista-Niño, E. Portilla-Fernandez, D. Vaughan, A. Danser, A. Roks, DNA damage: a Main determinant of vascular aging, *Int. J. Mol. Sci.* 17 (5) (2016) 748.
- [13] A.M. Cobb, S. Yusoff, R. Hayward, S. Ahmad, M. Sun, A. Verhulst, D. Haese, PC, Shanahan CM., Runx2 (runt-related transcription factor 2) links the DNA damage response to osteogenic reprogramming and apoptosis of vascular smooth muscle cells, *Arterioscler. Thromb. Vasc. Biol.* 41 (4) (2021) 1339–1357.
- [14] F. Bartoli-Leonard, F.L. Wilkinson, A. Schiro, F. Serracino Inglott, M.Y. Alexander, R. Weston, Loss of SIRT1 in diabetes accelerates DNA damage-induced vascular calcification, *Cardiovasc. Res.* 117 (3) (2021) 836–849.
- [15] A. Ciccia, S.J. Elledge, The DNA damage response: making it safe to play with knives, *Mol. Cell* 40 (2) (2010) 179–204.
- [16] A. Marechal, L. Zou, DNA damage sensing by the ATM and ATR kinases, *Cold Spring Harb. Perspect. Biol.* 5 (9) (2013), a12716.
- [17] C.J. Bakkenist, M.B. Kastan, DNA damage activates ATM through intermolecular autophosphorylation and dimer dissociation, *Nature*. 421 (6922) (2003) 499–506.
- [18] M. Qian, Z. Liu, L. Peng, X. Tang, F. Meng, Y. Ao, M. Zhou, M. Wang, X. Cao, B. Qin, Z. Wang, Z. Zhou, G. Wang, Z. Gao, J. Xu, B. Liu, Boosting ATM activity alleviates aging and extends lifespan in a mouse model of progeria, *eLife*. 7 (2018), e34836.
- [19] Y.M. Chung, S.H. Park, W.B. Tsai, S.Y. Wang, M.A. Ikeda, J.S. Berek, D.J. Chen, M. C. Hu, FOXO3 signalling links ATM to the p53 apoptotic pathway following DNA damage, *Nat. Commun.* 3 (2012) 1000.
- [20] A. Celeste, O. Fernandez-Capetillo, M.J. Kruhlak, D.R. Pilch, D.W. Staudt, A. Lee, R. F. Bonner, W.M. Bonner, A. Nussenzweig, Histone H2AX phosphorylation is dispensable for the initial recognition of DNA breaks, *Nat. Cell Biol.* 5 (7) (2003) 675–679.
- [21] L.J. Kuo, L.X. Yang, Gamma-H2AX - a novel biomarker for DNA double-strand breaks, *In Vivo*. 22 (3) (2008) 305–309.
- [22] P. Sanchis, C.Y. Ho, Y. Liu, L.E. Beltran, S. Ahmad, A.P. Jacob, M. Furmanik, J. Laycock, D.A. Long, R. Shroff, C.M. Shanahan, Arterial “inflammaging” drives vascular calcification in children on dialysis, *Kidney Int.* 95 (4) (2019) 958–972.
- [23] Y. Liu, I. Drozdov, R. Shroff, L.E. Beltran, C.M. Shanahan, Prelamin A accelerates vascular calcification via activation of the DNA damage response and senescence-associated secretory phenotype in vascular smooth muscle cells, *Circ. Res.* 112 (10) (2013) e99–e109.
- [24] J. Zhang, Q. Wu, L. Zhu, S. Xie, L. Tu, Y. Yang, K. Wu, Y. Zhao, Y. Wang, Y. Xu, X. Chen, S. Ma, S. Zhang, SERPINE2/PN-1 regulates the DNA damage response and radioresistance by activating ATM in lung cancer, *Cancer Lett.* 524 (2022) 268–283.
- [25] Z. Wang, X. Zhang, W. Li, Q. Su, Z. Huang, X. Zhang, H. Chen, C. Mo, B. Huang, W. Ou, J. Chen, G. Zhao, L. Chen, L. Shao, ATM/NEMO signaling modulates the expression of PD-L1 following docetaxel chemotherapy in prostate cancer, *J. Immunother. Cancer.* 9 (7) (2021), e1758.
- [26] M. Simon, M. Van Meter, J. Ablueva, Z. Ke, R.S. Gonzalez, T. Taguchi, M. De Cecco, K.I. Leonova, V. Kogan, S.L. Helfand, N. Neretti, A. Roichman, H.Y. Cohen, M.

- V. Meer, V.N. Gladyshev, M.P. Antoch, A.V. Gudkov, J.M. Sedivy, A. Seluanov, V. Gorbunova, LINE1 Derepression in aged wild-type and SIRT6-deficient mice drives inflammation, *Cell Metab.* 29 (4) (2019) 871–885.
- [27] H.G. Kim, M. Huang, Y. Xin, Y. Zhang, X. Zhang, G. Wang, S. Liu, J. Wan, A. R. Ahmadi, Z. Sun, S. Liangpunsakul, X. Xiong, X.C. Dong, The epigenetic regulator SIRT6 protects the liver from alcohol-induced tissue injury by reducing oxidative stress in mice, *J. Hepatol.* 71 (5) (2019) 960–969.
- [28] X. Tian, D. Firsanov, Z. Zhang, Y. Cheng, L. Luo, G. Tomblin, R. Tan, M. Simon, S. Henderson, J. Steffan, A. Goldfarb, J. Tam, K. Zheng, A. Cornwell, A. Johnson, J. Yang, Z. Mao, B. Manta, W. Dang, Z. Zhang, J. Vijg, A. Wolfe, K. Moody, B. K. Kennedy, D. Bohmann, V.N. Gladyshev, A. Seluanov, V. Gorbunova, SIRT6 is responsible for more efficient DNA double-strand break repair in long-lived species, *Cell.* 177 (3) (2019) 622–638.
- [29] S. Naiman, F.K. Huynh, R. Gil, Y. Glick, Y. Shahar, N. Toutou, L. Nahum, M. Y. Avivi, A. Roichman, Y. Kanfi, A.A. Gertler, T. Doniger, O.R. Ilkayeva, I. Abramovich, O. Yaron, B. Lerner, E. Gottlieb, R.A. Harris, D. Gerber, M. D. Hirschey, H.Y. Cohen, SIRT6 promotes hepatic beta-oxidation via activation of PPARalpha, *Cell Rep.* 29 (12) (2019) 4127–4143.
- [30] H.S. Kim, C. Xiao, R.H. Wang, T. Lahusen, X. Xu, A. Vassilopoulos, G. Vazquez-Ortiz, W.I. Jeong, O. Park, S.H. Ki, B. Gao, C.X. Deng, Hepatic-specific disruption of SIRT6 in mice results in fatty liver formation due to enhanced glycolysis and triglyceride synthesis, *Cell Metab.* 12 (3) (2010) 224–236.
- [31] C.A. Koczor, K.M. Saville, J.F. Andrews, J. Clark, Q. Fang, J. Li, R.Q. Al-Rahahleh, M. Ibrahim, S. McClellan, M.V. Makarov, M.E. Migaud, R.W. Sobol, Temporal dynamics of base excision/single-strand break repair protein complex assembly/disassembly are modulated by the PARP/NAD(+)/SIRT6 axis, *Cell Rep.* 37 (5) (2021), 109917.
- [32] Y. Fan, J. Cheng, Q. Yang, J. Feng, J. Hu, Z. Ren, H. Yang, D. Yang, G. Ding, Sirt6-mediated Nrf2/HO-1 activation alleviates angiotensin II-induced DNA DSBs and apoptosis in podocytes, *Food Funct.* 12 (17) (2021) 7867–7882.
- [33] J. Chen, Z. Liu, H. Wang, L. Qian, Z. Li, Q. Song, G. Zhong, SIRT6 enhances telomerase activity to protect against DNA damage and senescence in hypertrophic ligamentum flavum cells from lumbar spinal stenosis patients, *Aging (Albany NY)* 13 (4) (2021) 6025–6040.
- [34] M. Grootaert, A. Finigan, N.L. Figg, A.K. Uryga, M.R. Bennett, SIRT6 protects smooth muscle cells from senescence and reduces atherosclerosis, *Circ. Res.* 128 (4) (2021) 474–491.
- [35] F. Meng, M. Qian, B. Peng, L. Peng, X. Wang, K. Zheng, Z. Liu, X. Tang, S. Zhang, S. Sun, X. Cao, Q. Pang, B. Zhao, W. Ma, Z. Songyang, B. Xu, W. Zhu, X. Xu, B. Liu, Synergy between SIRT1 and SIRT6 helps recognize DNA breaks and potentiates the DNA damage response and repair in humans and mice, *eLife.* 9 (2020), e55828.
- [36] L. Onn, M. Portillo, S. Ilic, G. Cleitman, D. Stein, S. Kaluski, I. Shirat, Z. Slobodnik, M. Einav, F. Erdel, B. Akabayov, D. Toiber, SIRT6 is a DNA double-strand break sensor, *eLife.* 9 (2020), e51636.
- [37] S. Winnik, J. Auwerx, D.A. Sinclair, C.M. Matter, Protective effects of sirtuins in cardiovascular diseases: from bench to bedside, *Eur. Heart J.* 36 (48) (2015) 3404–3412.
- [38] J. Guo, Z. Wang, J. Wu, M. Liu, M. Li, Y. Sun, W. Huang, Y. Li, Y. Zhang, W. Tang, X. Li, C. Zhang, F. Hong, N. Li, J. Nie, F. Yi, Endothelial SIRT6 is vital to prevent hypertension and associated cardiorenal injury through targeting Nkx3.2-GATA5 signaling, *Circ. Res.* 124 (10) (2019) 1448–1461.
- [39] F. Yao, G. Yang, Y. Xian, G. Wang, Z. Zheng, Z. Jin, Y. Xie, W. Wang, J. Gu, R. Lin, The protective effect of hydroxytyrosol acetate against inflammation of vascular endothelial cells partly through the SIRT6-mediated PKM2 signaling pathway, *Food Funct.* 10 (9) (2019) 5789–5803.
- [40] Y. He, Y. Xiao, X. Yang, Y. Li, B. Wang, F. Yao, C. Shang, Z. Jin, W. Wang, R. Lin, SIRT6 inhibits TNF-alpha-induced inflammation of vascular adventitial fibroblasts through ROS and Akt signaling pathway, *Exp. Cell Res.* 357 (1) (2017) 88–97.
- [41] Y. Kida, M.S. Goligorsky, Sirtuins, cell senescence, and vascular aging, *Can. J. Cardiol.* 32 (5) (2016) 634–641.
- [42] M.L. Balestrieri, M.R. Rizzo, M. Barbieri, P. Paolisso, N. D'Onofrio, A. Giovane, M. Siniscalchi, F. Minicucci, C. Sardu, D. D'Andrea, C. Mauro, F. Ferraraccio, L. Servillo, F. Chirico, P. Caiazzo, G. Paolisso, R. Marfella, Sirtuin 6 expression and inflammatory activity in diabetic atherosclerotic plaques: effects of incretin treatment, *Diabetes.* 64 (4) (2015) 1395–1406.
- [43] X. Yang, A. Chen, Q. Liang, Q. Dong, M. Fu, X. Liu, S. Wang, Y. Li, Y. Ye, Z. Lan, J. Ou, L. Lu, J. Yan, Up-regulation of heme oxygenase-1 by celastrol alleviates oxidative stress and vascular calcification in chronic kidney disease, *Free Radic. Biol. Med.* 172 (2021) 530–540.
- [44] Z. Lan, A. Chen, L. Li, Y. Ye, Q. Liang, Q. Dong, S. Wang, M. Fu, Y. Li, X. Liu, Z. Zhu, J.S. Ou, X. Qiu, L. Lu, J. Yan, Downregulation of HDAC9 by the ketone metabolite beta-hydroxybutyrate suppresses vascular calcification, *J. Pathol.* 258 (2022) 213–226.
- [45] N.I. Ryabokon, R.I. Goncharova, G. Duburs, J. Rzeszowska-Wolny, A. 1,4-dihydropyridine derivative reduces DNA damage and stimulates DNA repair in human cells in vitro, *Mutat. Res.* 587 (1–2) (2005) 52–58.
- [46] T. Hou, Z. Cao, J. Zhang, M. Tang, Y. Tian, Y. Li, X. Lu, Y. Chen, H. Wang, F.Z. Wei, L. Wang, Y. Yang, Y. Zhao, Z. Wang, H. Wang, W.G. Zhu, SIRT6 coordinates with CHD4 to promote chromatin relaxation and DNA repair, *Nucleic Acids Res.* 48 (6) (2020) 2982–3000.
- [47] V. Turinetti, C. Giachino, Multiple facets of histone variant H2AX: a DNA double-strand-break marker with several biological functions, *Nucleic Acids Res.* 43 (5) (2015) 2489–2498.
- [48] E. Buraka, C.Y. Chen, M. Gavare, M. Grube, G. Makarenkova, V. Nikolajeva, I. Bisenieks, I. Bruvere, E. Bisenieks, G. Duburs, N. Sjakste, DNA-binding studies of AV-153, an antimutagenic and DNA repair-stimulating derivative of 1,4-dihydropyridine, *Chem. Biol. Interact.* 220 (2014) 200–207.
- [49] Y. Shiloh, Y. Ziv, The ATM protein kinase: regulating the cellular response to genotoxic stress, and more, *Nat. Rev. Mol. Cell Biol.* 14 (4) (2013) 197–210.
- [50] Z. Zhang, S.H. Ha, Y.J. Moon, U.K. Hussein, Y. Song, K.M. Kim, S. Park, H.S. Park, B. Park, A. Ahn, S. Lee, S.J. Ahn, J.R. Kim, K.Y. Jang, Inhibition of SIRT6 potentiates the anti-tumor effect of doxorubicin through suppression of the DNA damage repair pathway in osteosarcoma, *J. Exp. Clin. Cancer Res.* 39 (1) (2020) 247.
- [51] M.F. Lavin, S. Kozlov, ATM activation and DNA damage response, *Cell Cycle* 6 (8) (2007) 931–942.
- [52] S.E. Polo, A. Kaidi, L. Baskcomb, Y. Galanty, S.P. Jackson, Regulation of DNA-damage responses and cell-cycle progression by the chromatin remodelling factor CHD4, *EMBO J.* 29 (18) (2010) 3130–3139.
- [53] Q. Yao, P. Zhang, Y. Qi, S. Chen, B. Shen, Y. Han, Z. Yan, Z. Jiang, The role of SIRT6 in the differentiation of vascular smooth muscle cells in response to cyclic strain, *Int. J. Biochem. Cell Biol.* 49 (2014) 98–104.
- [54] W. Wei, X. Guo, L. Gu, J. Jia, M. Yang, W. Yuan, S. Rong, Bone marrow mesenchymal stem cell exosomes suppress phosphate-induced aortic calcification via SIRT6-HMGB1 deacetylation, *Stem Cell Res Ther* 12 (1) (2021) 235.
- [55] W. Li, W. Feng, X. Su, D. Luo, Z. Li, Y. Zhou, Y. Zhu, M. Zhang, J. Chen, B. Liu, H. Huang, SIRT6 protects vascular smooth muscle cell from osteogenic transdifferentiation via Runx2 in chronic kidney disease, *J. Clin. Invest.* 150051 (2021).
- [56] P. Zhang, A. Wang, H. Yang, L. Ai, H. Zhang, Y. Wang, Y. Bi, H. Fan, J. Gao, H. Zhang, J. Liu, Apelin-13 attenuates high glucose-induced calcification of MOVAS cells by regulating MAPKs and PI3K/AKT pathways and ROS-mediated signals, *Biomed. Pharmacother.* 128 (2020), 110271.
- [57] C. Lin, L. Zhang, B. Li, F. Zhang, Q. Shen, G. Kong, X. Wang, S. Cui, R. Dai, W. Cao, P. Zhang, Selenium-containing protein from selenium-enriched spirulina platensis attenuates high glucose-induced calcification of MOVAS cells by inhibiting ROS-mediated DNA damage and regulating MAPK and PI3K/AKT pathways, *Front. Physiol.* 11 (2020) 791.
- [58] A. Cardus, A.K. Uryga, G. Walters, J.D. Erusalimsky, SIRT6 protects human endothelial cells from DNA damage, telomere dysfunction, and senescence, *Cardiovasc. Res.* 97 (3) (2013) 571–579.
- [59] J. Sperlazza, M. Rahmani, J. Beckta, M. Aust, E. Hawkins, S.Z. Wang, Z.S. Zhu, S. Podder, C. Dumur, K. Archer, S. Grant, G.D. Ginder, Depletion of the chromatin remodeler CHD4 sensitizes AML blasts to genotoxic agents and reduces tumor formation, *Blood.* 126 (12) (2015) 1462–1472.